UCSB METHOD FOR BROADBAND GROUND MOTION FROM KINEMATIC SIMULATIONS OF EARTHQUAKES

Release Notes (V. 21.4)

Source Generator

We have revised the source generator of UCSB broadband kinematic simulation method (Liu*, et al.*, 2006; Schmedes*, et al.*, 2013; Crempien and Archuleta, 2015) by assuming that the realistic source model has a double-corner-frequency (DCF) source spectrum (Archuleta and Ji, 2016; Ji and Archuleta, 2020) rather than the single corner frequency (SCF) source spectrum used previously. The DCF spectrum used is defined as (Ji and Archuleta, 2020),

$$\Omega_0(f, f_{c1}, f_{c2}) = \frac{M_0}{\left[1+(\frac{f}{f_{c1}})^4\right]^{1/4}\left[1+(\frac{f}{f_{c2}})^4\right]^{1/4}} \quad (1)$$

As shown in Figure 1, the spectral amplitude of a DCF model remains constant for frequencies less than low corner frequency f_{c1}, decays as f^{-1} between f_{c1} and high corner frequency f_{c2}, and decays as f^{-2} for frequencies greater than f_{c2}.

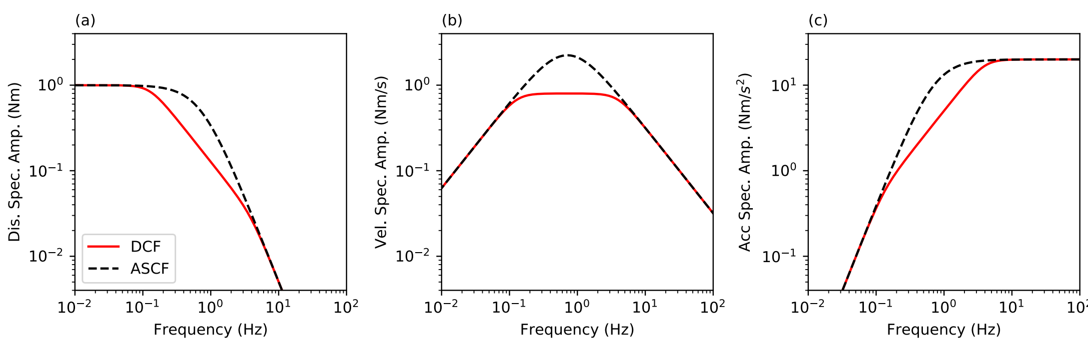

Figure 1. Comparison of a DCF spectral model (red line) and a single corner frequency spectral model with same low- and high-frequency asymptotes (ASCF, black dashed line). (a) displacement spectra. (b) velocity spectra and (c) acceleration spectra. Note that DCF model has less energy radiation between f_{c1} and f_{c2} than ASCF.

Ji and Archuleta (2020) introduce double-corner-frequency (DCF) source spectral models JA19_2S, which in conjunction with a stochastic ground-motion model, can reproduce the mean peak ground acceleration (PGA) and mean peak ground velocity (PGV) of the NGA West-2 database (Ancheta*, et al.*, 2014) for magnitudes 3.3 to 7.3. The JA19_2S scaling relation for corner frequency f_{c1} and f_{c2} are

$$\log(f_{c1}(\boldsymbol{M})) = \begin{cases} 1.474 - 0.415\,\boldsymbol{M} & 3.3 < \boldsymbol{M} \le 5.3 \\ 2.375 - 0.585\,\boldsymbol{M} & 5.3 < \boldsymbol{M} < 7.3 \end{cases} \quad (2a)$$

$$\log(f_{c2}(\boldsymbol{M})) = 3.250 - 0.5\boldsymbol{M} \quad (2b)$$

Here $\boldsymbol{M}$ denotes the moment magnitude. Ji and Archuleta (2020) found that the low corner frequency (f_{c1}) is associated with the rupture duration T_d as $T_d = 1/\pi f_{c1}$ and high corner frequency f_{c2} is correlated with average rise time T_R as $T_R = 0.8/f_{c2}$. If the fault length L (in km) of an earthquake is known, users may consider first using the empirical relations $T_d \sim L/2.8$ and $T_R \sim (0.08 - 0.1)T_d$ (Ji and Archuleta, 2022) to estimate T_d and T_R, and subsequently constraining f_{c1} and f_{c2}.

Following new rules are employed to constrain the spatial distributions of rupture front ($T(\vec{x}, t)$) and slip rate function for a given slip distribution.

a) Rather than giving a fixed average rupture velocity V_R as in previous versions of UCSB method, we perturb the ratio (γ) between rupture velocity (V_R) and shear wave velocity (V_s) on the fault so that the synthetic rupture duration (T_d, defined specially as 95% of seismic moment) is $1/\pi f_{c1}$. Note that V_s is not a constant.

b) Rupture front $T(\vec{x}, t)$ is modeled as $T_0(\vec{x}, t) + \delta(\vec{x}, t)$. $T_0(\vec{x}, t)$ defines the background rupture front from the hypocenter, calculated using the given rupture velocity distribution (i.e., γV_s) and a 2D finite difference travel-time solver. $\delta(\vec{x}, t)$ is the local perturbation. Based on the work of Gusev (2014) and Schmedes, *et al.* (2013), we let the spatial distribution of $\delta(\vec{x}, t)$ obey a k^{-1} spectral distribution and the values of $\delta(\vec{x}, t)$ satisfy the Rayleigh distribution with $\sigma = T_R/2$. The resulted rupture front is a tortuous, multiply connected ("lacy") fractal polyline that occupies a strip of finite width close to the slip-pulse width (Gusev, 2014) but has no correlation with the fault slip (Schmedes, *et al.*, 2013).

c) The default slip rate function at a point on the fault surface is modified Yoffe function, which is the convolution of a Yoffe function and a truncated cosine function (Schmedes, *et al.*, 2010). Its rise time $T_R(\vec{x})$ is equal to ${T_R}^0(\vec{x}) + T_P(\vec{x})$, where ${T_R}^0(\vec{x})$ and $T_P(\vec{x})$ are durations of corresponding Yoffe function and truncated cosine function respectively (Schmedes, *et al.*, 2010). Based on our previous dynamic study (Schmedes, *et al.*, 2013), we let ${T_R}^0(\vec{x})$ follow a $k^{-1.75}$ spatial distribution and the spatial correlation between ${T_R}^0(\vec{x})$ and fault slip $D(\vec{x})$ be 0.75. $T_P(\vec{x})$ follows a k^{-1} spatial distribution and the spatial correlation between T_P and fault slip $D(\vec{x})$ is negligible. We let the values of ${T_R}^0(\vec{x})$ obey a beta distribution (Liu, *et al.*, 2006), and initially normalize ${T_R}^0(\vec{x})$ so that their average $\overline{{T_R}^0}$ is equal to $1.2\overline{T_R}$. The default value of average $T_P(\vec{x})$, i.e., $\overline{T_P}$, is $0.2\overline{T_R}$.

d) In the last step, the values of $\overline{{T_R}^0}$ and $\overline{T_P}$ are further perturbed so that the amplitude spectrum of the cumulative moment rate function matches the target DCF spectral model, JA19_2S. We generate a pool of 25 different source realizations before selecting the best realization for further ground motion simulation.

Reference

Ancheta, T. D., R. B. Darragh, J. P. Stewart, E. Seyhan, W. J. Silva, B. S. J. Chiou, K. E. Wooddell, R. W. Graves, A. R. Kottke, D. M. Boore, T. Kishida, and J. L. Donahue (2014). NGA-West2 Database, *Earthquake Spectra,* **30,** no. 3, 989-1005. doi:10.1193/070913eqs197m.

Archuleta, R. J., and C. Ji (2016). Moment rate scaling for earthquakes 3.3M5.3 with implications for stress drop, *Geophys. Res. Lett.,* **43,** no. 23, 12004-12011.

Crempien, J. G. F., and R. J. Archuleta (2015). UCSB Method for Simulation of Broadband Ground Motion from Kinematic Earthquake Sources, *Seismol. Res. Lett.,* **86,** no. 1, 61-67. doi:10.1785/0220140103.

Gusev, A. A. (2014). Doubly Stochastic Earthquake Source Model: "Omega-Square" Spectrum and Low High-Frequency Directivity Revealed by Numerical Experiments, *Pure Appl. Geophys.,* **171,** no. 10, 2581-2599. doi:10.1007/s00024-013-0764-9.

Ji, C., and R. J. Archuleta (2020). Two empirical double-corner frequency source spectra and their physical implications, *Bull. Seismol. Soc. Am.* doi:10.1785/0120200238.

Ji, C., and R. J. Archuleta (2022). A Source Physics Interpretation of Nonself-Similar Double-Corner-Frequency Source Spectral Model JA19_2S, *Seismol. Res. Lett.,* **93,** no. 2A, 777-786. doi:10.1785/0220210098.

Liu, P. C., R. J. Archuleta, and S. H. Hartzell (2006). Prediction of broadband ground-motion time histories: Hybrid low/high-frequency method with correlated random source parameters, *Bull. Seismol. Soc. Am.,* **96,** no. 6, 2118-2130. doi:10.1785/0120060036.

Schmedes, J., R. J. Archuleta, and D. Lavallee (2010). Correlation of earthquake source parameters inferred from dynamic rupture simulations, *J. Geophys. Res.,* **115**. doi:10.1029/2009jb006689.

Schmedes, J., R. J. Archuleta, and D. Lavallee (2013). A kinematic rupture model generator incorporating spatial interdependency of earthquake source parameters, *Geophys. J. Int.,* **192,** no. 3, 1116-1131. doi:10.1093/gji/ggs021.